Effect of oral appliances on genioglossus muscle tonicity seen with diffusion tensor imaging: A pilot study

Hideo Shinagawa, DDS, PhD,[a] Emi Z. Murano, MD, PhD,[a] Jiachen Zhuo, MS,[b] Bennett Landman, PhD,[c] Rao P. Gullapalli, PhD,[b] Jerry L. Prince, PhD,[c] and Maureen Stone, PhD,[a] Baltimore, Maryland
UNIVERSITY OF MARYLAND BALTIMORE AND THE JOHNS HOPKINS UNIVERSITY

Objective. The purpose of this study was to examine whether the diffusion tensor imaging (DTI) technique can be used as a modality to represent the structural deformation in the in vivo genioglossus (GG) muscle fibers with oral appliances (OAs).
Study Design. Three healthy subjects were recruited for the pilot study. A custom-made OA, which is modified from a tongue retaining device (TRD), was constructed for each subject before the DTI acquisitions. Recordings were made with and without OAs to compare the GG muscle fiber deformation.
Result. DTI provided good resolution of tongue muscle fibers in vivo and successful isolation of each muscle fiber bundle. In particular, the GG muscle fiber deformation due to OAs was clearly visualized.
Conclusions. This DTI technique may be used not only to identify the individual myoarchitecture, but also to assess muscle fiber deformations in vivo, such as constriction, dilatation, and rotation with OAs. Clinical studies for OSA patients will be the next step. **(Oral Surg Oral Med Oral Pathol Oral Radiol Endod 2009;107:e57-e63)**

It is widely thought that the anatomical deformation of the upper airway muscles, especially the genioglossus (GG) muscle, might be important in the cause of obstructive sleep apnea (OSA).[1,2] In a cephalometric study,[3] OSA patients had hyoid bones that were located more inferiorly than normal and their tongues extended caudally toward the lower part of the pharynx. Endurance of GG muscles was found to decrease frequently with age, and was strongly associated with the increased prevalence of OSA.[4] Carrera et al.[5] found histologically that composition of fiber type (ie, types I and II) in GG muscles was different between healthy individuals and OSA patients. These changes influence fiber orientation, diameter, length, and distribution of muscle, fat, and connective tissues. However, there are no reports about the myoarchitecture of GG muscles in the in vivo tongue of OSA patients.

Oral appliances (OAs), such as a tongue retaining device (TRD)[6-8] and a mandibular advancement device (MAD),[9-11] are used as a therapeutic method for OSA patients. The TRD changes the tongue position and posture, whereas the MAD advances the mandible. Therefore, both of them help to compensate for impaired dilator muscle function (ie, posterior portion of the GG muscle) and to prevent the air passage from closing during sleep. Although the MAD is by far the most common OA in use today, the TRD is still an option for patients with temporomandibular dysfunction, edentulous dentition, or periodontal disease, as well as for those who cannot tolerate mandibular fixation.

Diffusion tensor imaging (DTI) was recently developed to investigate orientation and integrity of nerve structures in the central nervous system.[12-14] The method involves the estimation of the anisotropy in the tissues using the diffusion of water molecules, which is commonly known as Brownian motion. The diffusion characteristics depend on the component and structure of the tissues. An effective diffusion tensor is measured in each voxel by using a set of diffusion-weighted images. The eigenvectors and eigenvalues derived from the tensor provide information on the local tissue geometry. Tractography is a component post-processing method and is based on the assumption that the eigenvector with the largest eigenvalue (ie, the principal eigenvector) of the tensor coincides with the local fiber orientation.[15]

Some of this material was presented at the 85th General Session & Exhibition of the International Association for Dental Research in New Orleans. The research was supported by Postdoctoral Fellowships for Research Abroad of the Japan Society for the Promotion of Science (JSPS), and National Institute on Deafness and Other Communication Disorders (NIDCD) grant K99DC009279 and R01-01758.
[a]Department of Neural and Pain Sciences, University of Maryland Baltimore.
[b]Department of Diagnostic Radiology, University of Maryland Baltimore.
[c]Department of Biomedical Engineering, The Johns Hopkins University.
Received for publication Feb 26, 2008; returned for revision Oct 10, 2008; accepted for publication Nov 20, 2008.
1079-2104/$ - see front matter

doi:10.1016/j.tripleo.2008.11.022

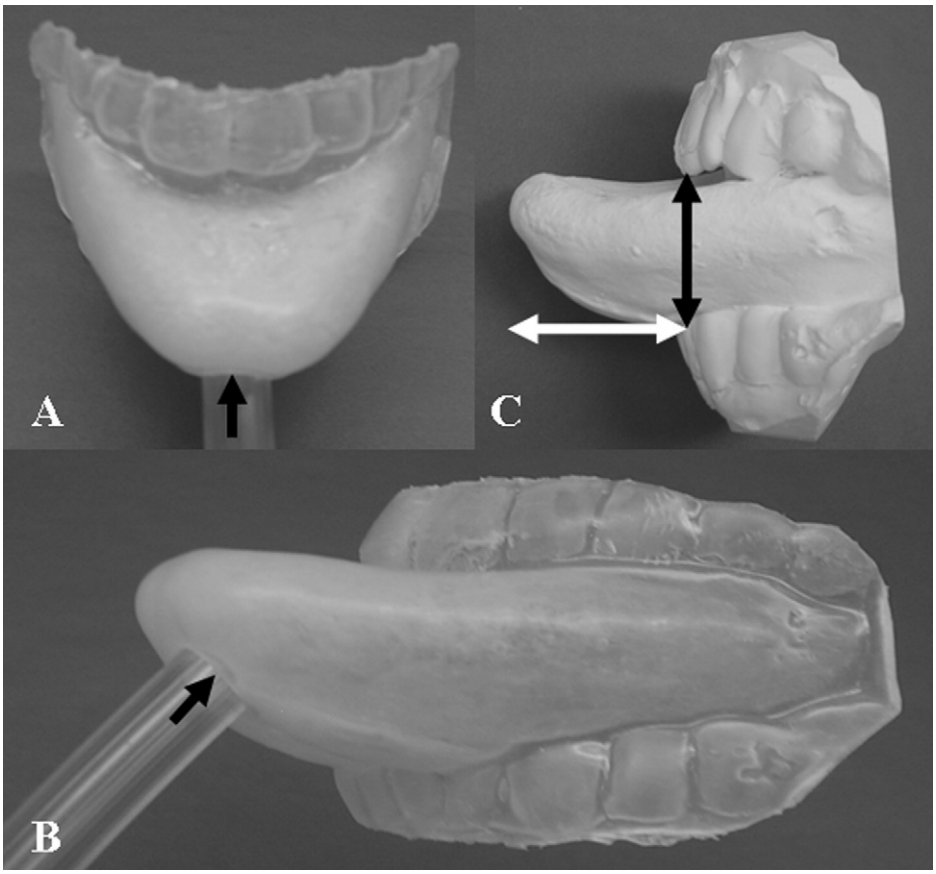

Fig. 1. Frontal (**A**) and oblique (**B**) views of a modified tongue retaining device (TRD), and lateral view (**C**) of a cast are shown. The black arrows in **A** and **B** denote a hole to which the vacuum hose is connected, thereby immobilizing the tongue and extracting saliva during MRI acquisitions. The cast (**C**) for fabricating the oral appliance (OA) was also used to measure the amount of tongue protrusion (*2-headed white arrow*) and mouth opening (*2-headed black arrow*), using a slide gauge.

The DTI technique has also been used for muscle fiber imaging and characterization.[16-23] In humans, the myocardial fiber orientation,[16] human calf muscle,[17] and the myoarchitecture of the human uterus[18] were successfully defined using the DTI technique. In the tongue, there have been some ex vivo studies in bovine,[19] mammalian,[20] and calf tongues.[21] In addition, the human tongue in vivo has been examined.[22-24] In this study, we apply the DTI technique to visualize the deformation of in vivo GG muscles with a custom-made OA, which is a modified TRD.

MATERIAL AND METHODS

Subjects

Three volunteers (2 males + 1 female, aged; 26 to 38 years), with no history of neurological or functional disorders, were recruited from the dental school staff for the pilot study. These data provide baseline normative effects of the OA to compare to subsequent studies of OSA patients. OSA patients should be able to tolerate these procedures absent neurological disorders that preclude holding the tongue still. The experimental procedures were approved by the Institutional Review Board of the University of Maryland. Written informed consent was obtained from the subjects before the study.

Material

Custom-made OAs were constructed of flexible polyvinyl material (Raintree ESSIX, Metairie, LA) for all subjects from plaster casts (see Fig. 1).[24] The OA shape was modified from the standard configuration of TRD to fix the tongue tightly because of the DT-MRI sensitivity to small motion. The subjects had silicone impressions made to transfer the tongue protrusion shape accurately to the cast. During the impression, each subject was instructed to protrude the tongue forward as much as possible with a comfortable mouth opening to create the shape of a tongue bulb to be built in the OA. This method of taking the impression was

designed to be comfortable for each subject and the quantitative effects of the protrusion on the tongue position and rotation were measured on MR images afterwards. The size of the tongue tip beyond the lower incisor (LI), which was measured in each cast (see Fig. 1, *C*) by using a slide gauge, was 24.6 mm for subject 1, 23.0 mm for subject 2 and 22.8 mm for subject 3. The finished tongue bulb was further modified by drilling a hole, with a diameter of about 10 mm, on the inferior surface, for suctioning saliva and creating a vacuum to fixate the tongue. The OA also fixed the jaws because it was attached to the upper and lower teeth by adhesive. The amount of the mouth opening was also measured at the distance between the upper and lower incisors in each cast (Fig. 1, *C*); 19.7 mm for subject 1, 20.6 mm for subject 2, and 25.5 mm for subject 3.

MRI acquisition

A 1.5-T MRI machine (Magnetom Avanto; Siemens, Erlangen, Germany) with 8 channel head and neck coil was used to obtain the MRI images. The subjects lay supine in the scanner. The head was fixed to the head coil with adhesive tape (AMD-Ritmed Inc., Plattsburgh, NY, USA). Recordings were made with and without the OA (hereafter, w/ OA and w/o OA). During the w/ OA task, a suction force of 150 to 200 mm Hg was used. A spin echo echo-planar imaging (EPI) pulse sequence with diffusion sensitizing gradients was applied in 6 collinear directions and b-value = 500 s/mm^2.[25] Other imaging parameters were the following: FOV = 200 mm, slice thickness = 3 mm (no gap), voxel size = 3.1 × 3.1 × 3.0 mm, matrix size = 64 × 64, repetition time (TR) = 5000 ms, echo time (TE) = 66 ms, 4 averages. Twenty-three to 28 axial slices parallel to the skin surface of the mandible were chosen for each subject to cover the whole tongue volume. Total acquisition time was approximately 3 minutes.

T1- and T2-weighted high-resolution MRI images were also taken of sagittal, axial, and coronal sections, using the following parameters: T1: FOV = 160 mm, TR = 600 ms, TE = 14 ms, voxel size = 0.8 × 0.8 × 3.0 mm, matrix size = 256; T2: FOV = 160 mm, TR = 3000 ms, TE = 99 ms, voxel size = 0.8 × 0.6 × 3.0 mm, matrix size = 256. The high-resolution axial slices, matched in thickness and position to the DT slices, were used as anatomical references. In addition, the midsagittal slices w/ and w/o the device were used for morphological measurements.

Data analysis

The analysis and visualization of tongue fiber tracking were performed using dTV-II implemented in VOLUME-ONE software (University of Tokyo, http://www.ut-radiology.umin.jp). The threshold for the fiber tracking was set at fractional anisotropy (FA) greater than 0.18. Regions of interest (ROIs) for GG muscle fiber tracking were chosen manually, using both T2 axial and coronal images.[26] In order to display 3D fiber

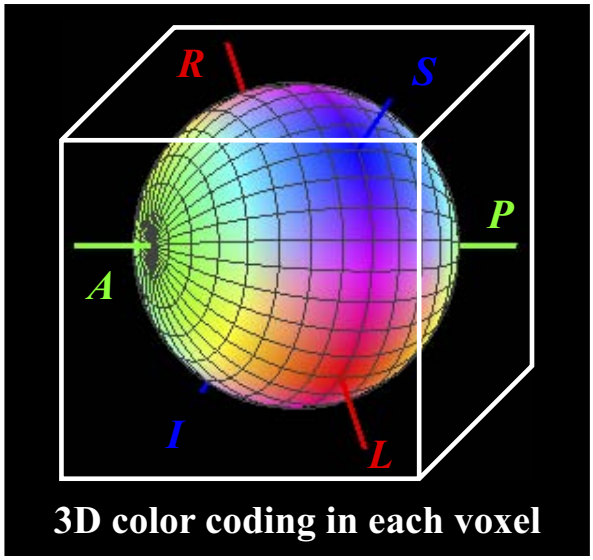

Fig. 2. Three-dimensional color-coding method is shown. In order to display 3D fiber tracking (ie, tractography), the directions of the x, y, and z coordinates within each voxel were calculated and converted to eigenvector coordinates. The fiber direction within each voxel was color-coded by the direction of the principal eigenvector. The fiber orientation was depicted using the 3D color-coding method: green is horizontal (anterior–posterior); blue is vertical (superior-inferior); and red is transverse (left-right).

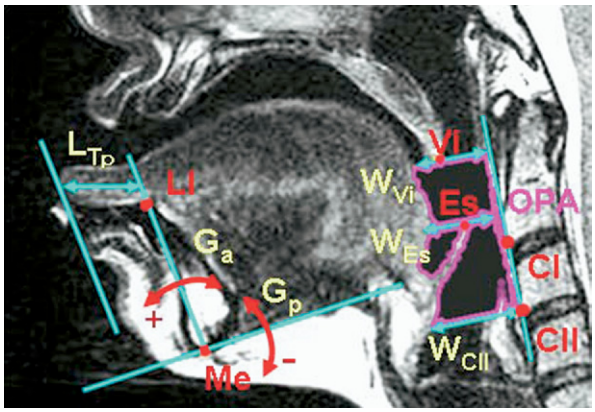

Fig. 3. Reference points for oral measurements: the lower incisor (LI), menton (Me), the most inferior velar point (Vi), the most superior epiglottal point (Es), and the inferior edge of the second cervical vertebrae (CII). Measurements (see Table I) included tongue protrusion length (L_{Tp}), velopharyngeal width (W_{Vi}), oropharyngeal width (W_{Es}), oro-hypopharynx area (OPA), and angles (Ga and Gp).

Table I. Summary of the measurements, abbreviations, and definitions

Measurements	*Abbreviations*	*Definitions*
Length, widths, and area		
(1) Tongue protrusion length	L_{Tp}	Length between the LI-Me line and the parallel line that touches the tongue tip
(2) Velopharyngeal width	Wvi	Width at the height of the most inferior velar point (Vi)
(3) Oropharyngeal width	W_{Es}	Width at the height of the most superior epiglottal point (Es)
(4) Oro-hypopharynx area	OPA	Area between Wvi and W_{CII}*
Angles		
(5) Anterior GG muscle	Ga	Angle between the front edge of GG muscle and the LI-Me line
(6) Posterior GG muscle	Gp	Angle between the bottom edge of GG muscle and the perpendicular to the LI-Me line
(7) Spread of GG muscle	Sp	Angle between the Ga and Gp

*Hypopharyngeal width (W_{CII}); Width at the height of the inferior edge of the second cervical vertebrae (CII). The data were not shown.

tracking (ie, tractography), the principal eigenvector in each voxel was color-coded as demonstrated by a 3D colored sphere (Fig. 2):[15,27] green is horizontal (anterior-posterior); blue is vertical (superior-inferior); and red is transverse (left-right).

Measurements

Fig 3 shows the reference points, lines, and angles used for the 7 measurements shown in Table I.[28-31] The reference points shown in red at Fig. 3 are as follows: LI, the lower incisor; Me, Menton; Vi, the most inferior velar point; Es, the most superior epiglottal point; CI, the inferior edge of the first cervical vertebrae; and CII, the inferior edge of the second cervical vertebrae. Each line through the pharynx (ie, W_{Vi}, W_{Es}, and W_{CII}) was drawn perpendicular to the line between the CI and CII. The measurements were performed by one rater 3 times at a few days' interval for each image by using ImageJ version 1.38p software (NIMH, http://rsb.info.nih.gov/ij/). The averaged values (Mean) and standard deviation (SD) of the 3 trials were calculated. To assess the intra-rater variability, intra-class correlation coefficient (ICC) and the coefficient of variation (CV) were also calculated. The analysis yielded ICC greater than 0.95 and CV between 0.2% and 3.0% for all measurements.

RESULTS

Configuration of the tongue muscles without OA

DTI provided good resolution of all tongue muscles and successful isolation of GG muscle fibers to reveal OA-induced rotation, and subject differences. Fig. 4, *A* shows the tongue in subject 1 w/o OA. The fiber tracks of multiple muscles are shown in Fig. 4, *B*. Superior longitudinalis has circumferential fibers coursing along the upper surface (green) and angling downward at the pharyngeal surface (blue). In the tip, the transverse bundles (red) of transverses are seen between the vertical fibers (blue) of GG-anterior (GGA). Inferior longitudinalis originates at the tongue tip (green) and courses back through GG. The fan shape of GG, originating at the mandible, is visualized as half blue (vertical) and half green (horizontal). The horizontal fibers of geniohyoid are at the bottom. Thus, the relation between intrinsic and extrinsic muscle fibers in vivo was correctly observed.

Comparisons of GG muscle fiber orientation without and with OA

Fig 5 shows the tongue fiber orientation w/o and w/ OA, respectively, in the midsagittal slice of subject 1. The orientation of the GG muscle, which is fan shaped, clearly differs in the 2 conditions. More fibers of GG are vertical w/ OA (blue). The tongue protrusion seen in the MRI images is 21.6 mm for this subject. This is similar to the protrusion measured from the cast to create the OA.

Morphological comparisons between the without and with OA conditions

Morphological measurements showed that all tongues were protruded forward (ie, L_{TP}) in the w/ OA condition by about 2 cm (Table II). Marked enlargements were observed in pharyngeal width (ie, W_{Vi} and W_{Es}) and area (ie, OPA) in subjects 1 and 2 w/ OA, but not subject 3 (Table II). The GG muscle fiber angles for w/ and w/o OA are also shown in Table II. All the angles, especially in subjects 1 and 2, were rotated upward into a more oblique orientation w/ OA. Subject 3 had less rotation than the others (Table II). Also none of the subjects had more than 3 degrees change in Sp, which meant no change in radial spread of GG muscle fibers.

DISCUSSION

This is the first study to depict the GG muscle deformation effects of OAs, using the DTI technique. The technique successfully extracted the complex structure of intrinsic and extrinsic muscle fibers in vivo (Fig. 4) and correctly visualized fiber deformation of the GG muscles (Fig. 5). The data appear cluttered in

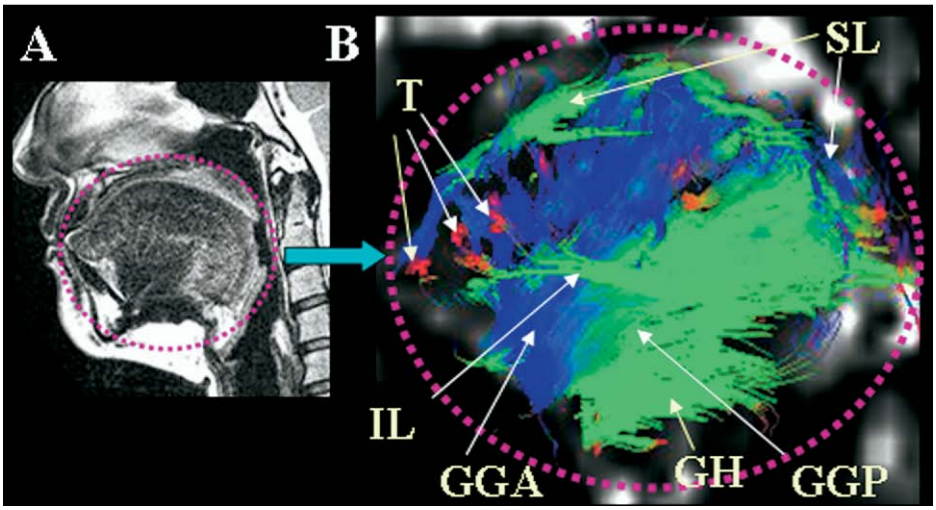

Fig. 4. A midsagittal slice of the head is shown with the tongue circled (**A**). The tractography for the area circled in **A** is shown in **B**. Muscle fibers include genioglossus-anterior (GGA), genioglossus-posterior (GGP), inferior longitudinalis (IL), superior longitudinalis (SL), geniohyoid (GH), and transversalis (T).

Table II. Measurements for each subject

(A)										
Subject		*(2) W_{Vi}*			*(3) W_{Es}*			*(4) OPA*		
Mean ± SD	*(1) L_{Tp}*	*w/o OA*	*w/OA*	*Ratio*	*w/o OA*	*w/OA*	*Ratio*	*w/o OA*	*w/OA*	*Ratio*
1	21.6 ± 0.2	5.6 ± 0.12	17.6 ± 0.15	3.1 ± 0.08	6.4 ± 0.15	16.4 ± 0.06	2.6 ± 0.07	294.9 ± 4.11	755.5 ± 6.52	2.6 ± 0.01
2	19.4 ± 0.36	10.4 ± 0.12	20.4 ± 0.12	2.0 ± 0.02	14.9 ± 0.12	24.3 ± 0.1	1.6 ± 0.02	439.8 ± 7.70	622.3 ± 2.55	1.4 ± 0.03
3	19.3 ± 0.15	9.2 ± 0.23	7.5 ± 0.06	0.8 ± 0.03	10.5 ± 0.06	9.3 ± 0.12	0.9 ± 0.01	360.5 ± 3.83	417.6 ± 5.41	1.2 ± 0.03

(B)									
Subject	*(5) Ga*			*(6) Gp*			*(7) Sp*		
Mean ± SD	*w/o OA*	*w/OA*	*Diff*	*w/o OA*	*w/OA*	*Diff*	*w/o OA*	*w/OA*	*Ratio*
1	−14.8° ± 0.65	+15.2° ± 0.29	30.0° ± 0.70	−22.2° ± 0.25	+10.2° ± 0.36	32.4° ± 0.12	97.4° ± 0.81	95.0° ± 0.25	2.4° ± 0.59
2	−2.8° ± 0.29	+9.5° ± 0.25	12.3° ± 0.36	+11.8° ± 0.72	+27.1° ± 0.66	15.3° ± 0.26	75.4° ± 0.71	72.4° ± 0.57	3.0° ± 0.70
3	−8.4° ± 0.50	−3.5° ± 0.62	4.93° ± 0.49	−30.4° ± 0.69	−24.8° ± 0.76	5.56° ± 0.51	112.0° ± 0.42	111.3° ± 0.76	0.63° ± 0.80

Ratio is w/OA divided by w/o OA. *Diff* is w/OA minus w/o OA. The scales are mm for L_{Tp}, W_{Vi}, and W_{Es}, mm^2 for OPA, and degrees (°) for Ga, Gp and Sp. Clockwise is − and counter clockwise is +.

Fig. 4 because fibers for the entire 3D volume are superimposed; nonetheless, muscle fibers can be visually extracted. In Fig. 5, GG muscle fibers were especially well visualized because they are bundled at their origin, which led to very effective seeding for fiber tracking. The rotation of GG muscle fibers between the w/ and w/o OA was shown clearly. In particular, the number of vertical GG fibers increased noticeably w/ OA, but the spread of fibers remained constant (Fig. 5). This was especially true in subjects 1 and 2.

The OA produced tongue rotation, and increased the percentage of vertical GG fibers in subjects 1 and 2, not in subject 3. The degree of rotation was approximately consistent with the percent of enlargements in the upper airway. Subject 1 had almost twice as much rotation and enlargement as subject 2 (see Table II). Subject 3 had little rotation and enlargement in comparison with subjects 1 and 2. In this data set GG muscle rotation was the most salient effect of OAs.

Fujita et al.[32] stated that there are 2 types of mechanisms to protrude the tongue forward: one is the elongation of the tongue, which is done by co-contraction of verticalis (V) and transversalis (T) muscles, and the other is the tongue body protrusion, which is generated by activating the posterior portion of the GG muscle. In this study, subject 1 and 2 protrude their tongues forward bodily and the tongue dorsa were flat. On the other hand, subject 3 elongated his tongue narrowly. These results were also correlated to the amounts of mouth opening (ie, 19.7 mm for subject 1, 20.6 mm for

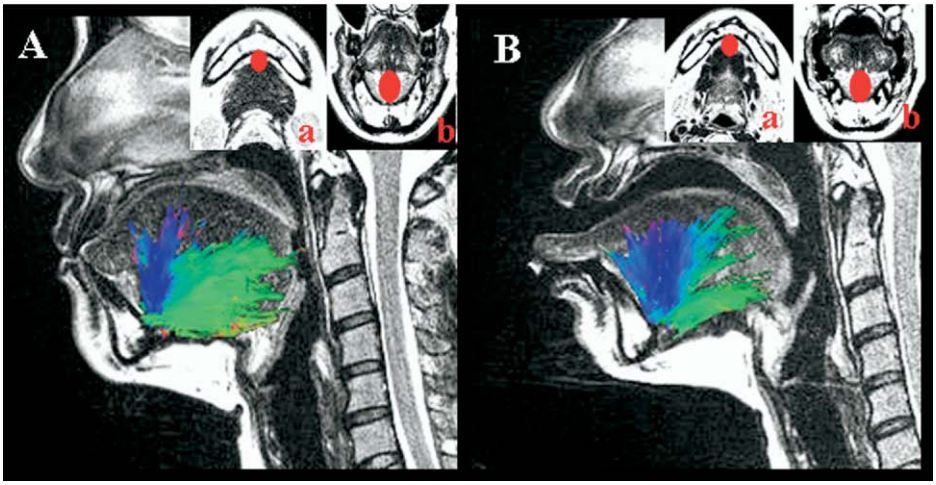

Fig. 5. GG muscle fiber tracking in subject 1 w/o OA (**A**) and w/ OA (**B**). Regions of interest (ROIs) for GG muscle fiber tracks were placed by using T2 axial (a) and coronal (b) images (see areas colored with red). The GG muscle fibers were superimposed on the T2 midsagittal image. The fiber orientation is more vertical in **B** than **A**.

subject 2, and 25.5 mm for subject 3). The tongues in subject 1 and 2 might be protruded by the activation of the GG muscles, whereas the tongue in subject 3 might be protruded by the activation of V and T muscles when the impressions were taken. This might be a hint to fabricate effective TRDs.

However, this study had several limitations. First, all participants were healthy volunteers and awake, unlike the conditions under which OSA occurs. Second, the parameters such as the amount of tongue protrusion and mouth opening, and the shape of the protruded tongue were not strictly defined for each subject when the OAs were fabricated. Third, tractography was performed by one rater and the intra-rater reproducibility was not accessed. Further studies with OSA patients who have had successful or unsuccessful OA treatment, and a larger sample size, are needed to fully evaluate effectiveness of the tongue response to OAs.

In conclusion, GG fiber orientation changes w/ OA were visualized in vivo with the noninvasive and nonradiative DTI technique. The DTI has the potential to reveal the deformation of the myoarchitecture of the tongue muscles in vivo. This study showed that DTI may be applied to OSA research to help us understand the fiber deformation such as compression, expansion and translation in tongue muscles in OSA patients in vivo, since it is possible to clarify the changes in GG muscle fiber orientation due to OAs.

We thank Dr. Stuart Josell and Mr. Harvey Lawson of the Department of Orthodontics at the University of Maryland, Dental School for their consultation about oral devices.

REFERENCES

1. Tsuiki S, Ono T, Kuroda T. Mandibular advancement modulates respiratory-related genioglossus electromyographic activity. Sleep Breath 2000;4:53-8.
2. BuSha BF, Strobel RJ, England SJ. The length-force relationship of the human genioglossus in patients with obstructive sleep apnea. Respir Physiol Neurobiol 2002;130:161-8.
3. Tangugsorn V, Krogstad O, Espeland L, Lyberg T. Obstructive sleep apnoea: multiple comparisons of cephalometric variables of obese and non-obese patients. J Craniomaxillofac Surg 2000;28:204-12.
4. Oliven A, Carmi N, Coleman R, Odeh M, Silbermann M. Age-related changes in upper airway muscles morphological and oxidative properties. Exp Gerontol 2001;36:1673-86.
5. Carrera M, Barbé F, Sauleda J, Tomás M, Gómez C, Agustí AG. Patients with obstructive sleep apnea exhibit genioglossus dysfunction that is normalized after treatment with continuous positive airway pressure. Am J Respir Crit Care Med 1999; 159:1960-6.
6. Cartwright RD. Predicting response to the tongue retaining device for sleep apnea syndrome. Arch Otolaryngol 1985; 111:385-8.
7. Ono T, Lowe AA, Ferguson KA, Pae EK, Fleetham JA. The effect of the tongue retaining device on awake genioglossus muscle activity in patients with obstructive sleep apnea. Am J Orthod Dentofacial Orthop 1996;110:28-35.
8. Higurashi N, Kikuchi M, Miyazaki S, Itasaka Y. Effectiveness of a tongue-retaining device. Psychiatry Clin Neurosci 2002;56: 331-2.
9. Sadan A, Novoselsky A, Rogers WA. An alternative technique for mandibular advancement prosthesis fabrication. J Prosthodont 1998;7:40-4.
10. Yoshida K. Effect of a prosthetic appliance for treatment of sleep apnea syndrome on masticatory and tongue muscle activity. J Prosthet Dent 1998;79:537-44.
11. Barthlen GM, Brown LK, Wiland MR, Sadeh JS, Patwari J, Zimmerman M. Comparison of three oral appliances for treatment of severe obstructive sleep apnea syndrome. Sleep Med 2000;1:299-305.

12. Horsfield MA, Jones DK. Applications of diffusion-weighted and diffusion tensor MRI to white matter diseases—a review. NMR Biomed 2002;15:570-7.
13. Bammer R. Basic principles of diffusion-weighted imaging. Eur J Radiol 2003;45:169-84.
14. Hagmann P, Thiran JP, Jonasson L, Vandergheynst P, Clarke S, Maeder P, et al. DTI mapping of human brain connectivity: statistical fibre tracking and virtual dissection. Neuroimage 2003;19:545-54.
15. Mori S, van Zijl PC. Fiber tracking: principles and strategies—a technical review. NMR Biomed 2002;15:468-80.
16. Reese TG, Weisskoff RM, Smith RN, Rosen BR, Dinsmore RE, Wedeen VJ. Imaging myocardial fiber architecture in vivo with magnetic resonance. Magn Reson Med 1995;34:786-91.
17. Sinha S, Sinha U, Edgerton VR. In vivo diffusion tensor imaging of the human calf muscle. J Magn Reson Imaging 2006;24: 182-90.
18. Weiss S, Jaermann T, Schmid P, Staempfli P, Boesiger P, Niederer P, et al. Three-dimensional fiber architecture of the nonpregnant human uterus determined ex vivo using magnetic resonance diffusion tensor imaging. Anat Rec A Discov Mol Cell Evol Biol 2006;288:84-90.
19. Wedeen VJ, Reese TG, Napadow VJ, Gilbert RJ. Demonstration of primary and secondary muscle fiber architecture of the bovine tongue by diffusion tensor magnetic resonance imaging. Biophys J 2001;80:1024-8.
20. Napadow VJ, Chen Q, Mai V, So PT, Gilbert RJ. Quantitative analysis of three-dimensional-resolved fiber architecture in heterogeneous skeletal muscle tissue using nmr and optical imaging methods. Biophys J 2001;80:2968-75.
21. Kim S, Chi-Fishman G, Barnett AS, Pierpaoli C. Dependence on diffusion time of apparent diffusion tensor of ex vivo calf tongue and heart. Magn Reson Med 2005;54:1387-96.
22. Gilbert RJ, Napadow VJ. Three-dimensional muscular architecture of the human tongue determined in vivo with diffusion tensor magnetic resonance imaging. Dysphagia 2005;20:1-7.
23. Gaige TA, Benner T, Wang R, Wedeen VJ, Gilbert RJ. Three dimensional myoarchitecture of the human tongue determined *in vivo* by diffusion tensor imaging with tractography. J Magn Reson Imaging 2007;26:654-61.
24. Shinagawa H, Murano EZ, Zhuo J, Landman B, Gullapalli RP, Prince JL, et al. Human tongue muscle fiber tracking during rest and tongue protrusion with oral appliance: a preliminary study with diffusion tensor imaging. Acoust Sci & Tech 2008;29: 291-4.
25. Pierpaoli C, Jezzard P, Basser PJ, Barnett A, Di Chiro G. Diffusion tensor MR imaging of the human brain. Radiology 1996;201:637-48.
26. How SC, McConnell AK, Taylor BJ, Romer LM. Acute and chronic responses of the upper airway to inspiratory loading in healthy awake humans: an MRI study. Respir Physiol Neurobiol 2007;157:270-80.
27. Jones DK, Simmons A, Williams SC, Horsfield MA. Non-invasive assessment of axonal fiber connectivity in the human brain via diffusion tensor MRI. Magn Reson Med 1999;42:37-41.
28. Gao X, Otsuka R, Ono T, Honda E, Sasaki T, Kuroda T. Effect of titrated mandibular advancement and jaw opening on the upper airway in nonapneic men: a magnetic resonance imaging and cephalometric study. Am J Orthod Dentofacial Orthop 2004;125:191-9.
29. Trudo FJ, Gefter WB, Welch KC, Gupta KB, Maislin G, Schwab RJ. State-related changes in upper airway caliber and surrounding soft-tissue structures in normal subjects. Am J Respir Crit Care Med 1998;158:1259-70.
30. Vialet R, Nau A, Chaumoître K, Martin C. Effects of head posture on the oral, pharyngeal and laryngeal axis alignment in infants and young children by magnetic resonance imaging. Paediatr Anaesth 2008;18:525-31.
31. Fusco G, Macina F, Macarini L, Garribba AP, Ettorre GC. Magnetic resonance imaging in simple snoring and obstructive sleep apnea-hypopnea syndrome. Radiol Med 2004;108:238-54.
32. Fujita S, Dang J, Suzuki N, Honda K. A computational tongue model and its clinical application. Oral Science International 2007;5:97-109.

Reprint requests:

Hideo Shinagawa, DDS, PhD
Department of Neural and Pain Sciences
University of Maryland, Baltimore
650 W Baltimore St.
Baltimore, MD 21201
HShinagawa@umaryland.edu